Material Transfer in Turbulent Gas Streams. Effect of Turbulence on Macroscopic Transport from Spheres

R. A. S. BROWN, KAZUHIKO SATO, and B. H. SAGE
California Institute of Technology, Pasadena, Calif.

Experimental information concerning material transport from spherical surfaces is extensive. Morse (*29*) studied the sublimation of iodine to a gas stream, and his work formed the background of Langmuir's development (*21*) of a classic expression to describe evaporation from spheres to stagnant air. Frössling (*8, 9*) studied experimentally the evaporation from drops to a flowing gas stream and also developed theoretical analyses of such a process. Hsu (*14*) investigated the effect of the shape of a drop upon its rate of evaporation. Linton and Sherwood (*24*) studied mass transfer from solid shapes to water.

Ingebo (*16, 17*) investigated the evaporation from cork spheres. Powell (*31*) studied the transport of water from linen and vellum-covered spheres, cylinders, and plane surfaces. Maisel and Sherwood (*26*) also studied material transport from these solid shapes. Ranz and Marshall (*32*), Bedingfield and Drew (*1*), and Hsu (*14*) found the wet-bulb temperature of drops to be relatively independent of the Reynolds number of the flow. However, the evaporation from drops as studied by Ranz and Marshall (*32*), Frössling (*9*), and Hsu (*14*) is a different process from the evaporation from spherical surfaces as studied by Ingebo (*16, 17*). In the case of drops there is a marked internal circulation (*15*); in the case of porous spheres, it is only as the result of conduction and relatively slow radial migration of the evaporating liquid that energy is transported from one part of the sphere to another. For this reason it is to be expected that much larger temperature differences would exist, from point to point on the surface of a porous sphere from which a liquid is evaporating, than are encountered in the case of a drop, particularly if the porous sphere is composed of a material of relatively low thermal conductivity.

The effect of level of turbulence upon the rate of evaporation has not been studied in great detail. Maisel and Sherwood (*27*) studied the effects of level and scale of turbulence upon the evaporation from cylinders and spheres and found a significant effect of the level of turbulence upon the transport rate. Comings, Clapp, and Taylor (*4*) studied the effect of induced turbulence upon material transport from a cylinder. They also found a marked increase in transport with an increase in level of turbulence.

For the present investigation a porous ceramic sphere 0.5 inch in diameter was supported upon a small tube through which *n*-heptane was introduced. The experimental measurements were made in two parts. The first part involved the evaluation of the surface temperature of the ceramic sphere as a function of polar angle, velocity, and level of turbulence of the flow of air, and included the evaluation of the rate of evaporation of *n*-heptane as a function of these variables. The second part of the experimental measurements comprised a more extended investigation of the rate of evaporation of *n*-heptane as a function of the velocity and level of turbulence of the flow. Measurements of the rate of evaporation were made at levels of turbulence between 0.01 and 0.15 fractional longitudinal turbulence for air stream velocities between 4 and 32 feet per second. The level of turbulence is expressed in this paper as the ratio of the root-mean-square of the fluctuating longitudinal velocity to the average macroscopic velocity of the stream.

ANALYSIS

The methods of analysis used by Frössling (*9*), Ranz and Marshall (*32*), Hsu (*14*), and Schlinger (*37*), which apply an energy balance to the evaporation of liquid from the surface of a sphere, were followed. Under steady conditions, the local energy balance at the interface is expressed by:

$$\mathring{Q} = -\mathring{m}_k (H_{g,i,k} - H_{l,t,k}) = -\mathring{m}_k [L_k + C_{p,l,k}(t_i^* - t_l)] \quad (1)$$

Negative signs arise from the convention that the evaporation from the interface constitutes a negative weight rate of flow. Equation 1 is based upon the assumptions of local equilibrium (*19*) at the transport surface and ideal solution in the gas phase (*22*). The total thermal transport to the sphere results from the energy addition by conduction through the boundary flows of the air stream and through the supporting injection tube, as well as from radiation, as indicated in the following expression:

$$\begin{aligned}\mathring{\underline{Q}} &= -\mathring{\underline{m}}_k [L_k + C_{p,l,k}(t_i^* - t_l)] - \mathring{\underline{Q}}_t - \mathring{\underline{Q}}_r \\ &= -\mathring{\underline{m}}_k [L_k + C_{p,l,k}(t_i^* - t_l)] + (k_l A_l + k_t A_t + \\ &\quad k_w A_w)\left(\frac{dt_t}{dx}\right)_{n=0} - A_i \beta (T_i^4 - T_{sr}^4) \frac{1}{\frac{1}{\epsilon_{sp}} + \frac{1}{\epsilon_{sr}} - 1}\end{aligned} \quad (2)$$

Following the vectorial convention, $\mathring{\underline{Q}}$ is a negative quantity when the thermal transfer is to the surface. The radiant transfer was evaluated from the emissivity coefficient recommended by McAdams (*25*). In most instances the radiation amounted to several per cent of the total energy transport (*3*). The remaining transport by convection was somewhat below values reported by McAdams (*25*).

In Equation 2 subscripts *t* and *w* refer, respectively, to the injection tube, and the thermocouple wire contained in the supporting tube. Subscript *l* refers to liquid *n*-heptane under the conditions existing in the injection tube. The values of the several terms set forth in Equation 2 are available (*3*).

The Nusselt number for convective thermal transfer is defined by

$$\mathrm{Nu} = \frac{hd}{k} = \frac{2hr}{k_i} = \frac{2\mathring{\underline{Q}}_r}{(t_i^* - t_\infty)k_i} = \frac{2\mathring{\underline{Q}}_r}{A_i(t_i^* - t_\infty)k_i} \quad (3)$$

Combination of Equations 2 and 3 and utilization of the concept of potential theory for the flow external to the boundary layer (*9*) results in

$$\mathrm{Nu} = \phi(\mathrm{Pr}, \mathrm{Re}) = 2[1 + K\mathrm{Pr}^{1/3}\mathrm{Re}^{1/2}] \quad (4)$$

The analogous dimensionless function for mass transfer, the Sherwood number (*34*), may be defined as

$$\mathrm{Sh} = m_c l \frac{P}{D_{M,k}} = 2 m_c r \frac{P}{D_{M,k}} \quad (5)$$

In the case of material transfer from spheres, the following expression may be used to evaluate the Sherwood number

for a binary system if fugacity is used as the driving potential for diffusion:

$$\mathrm{Sh} = -\frac{\overset{\circ}{m}_k b_k T}{2\pi r D_{M,k} Z \left(\frac{f_k^0}{P}\right) \ln\left(\frac{n_{ji}}{n_{j\infty}}\right)} \tag{6}$$

Equation 6 also assumes that the gas phase is an ideal solution (*22*). The minus sign in Equation 6 arises from the sign of the logarithm in the denominator. Strictly speaking subscript k or other component designation should always be used with the Sherwood number. However, in the interest of simplicity it has been omitted in this discussion. In this analysis the force-length-time system of dimensions was employed.

Total rate of evaporation from a sphere may be predicted to a reasonable degree of approximation from

$$\begin{aligned}\overset{\circ}{m}_k &= -\frac{4\pi r D_{M,k} Z}{b_k T}\left(\frac{f_k^0}{P}\right)\ln\left(\frac{n_{ji}}{n_{j\infty}}\right)[1 + K\,\mathrm{Re}_\alpha \mathrm{Sc}^{1/3}] \\ &= -\frac{2\pi r D_{M,k} Z}{b_k T}\left(\frac{f_k^0}{P}\right)\ln\left(\frac{n_{ji}}{n_{j\infty}}\right)\mathrm{Sh}\end{aligned} \tag{7}$$

The relationship shown in Equation 7 is similar to the expressions developed by Frössling (*9*) and used by Ranz and Marshall (*32*) and Hsu (*14*) to systematize the experimental data for the evaporation from spherical drops. Equation 7 permits the rate of material transport to be predicted from the molecular properties of the phase and the conditions of flow. In Equation 7 fugacity (*23*) is assumed as the driving potential for diffusion of component k in the gas phase adjacent to the surface of the sphere. The choice of fugacity as a driving potential is based upon simple treatments of the principles of irreversible thermodynamics (*10*), which do not apply at a distance from equilibrium. However, it has been found experimentally (*36*) that for hydrocarbons the Maxwell diffusion coefficient can be used satisfactorily with fugacity as the driving potential rather than partial pressure. Since fugacity was employed as the driving potential in the basic measurements used to establish the Maxwell diffusion coefficients (*36*), it was adopted as the driving potential for this discussion. It is assumed that the phase is an ideal solution (*22*), but not necessarily a perfect gas.

For the purposes of this discussion the Reynolds number is defined as

$$\mathrm{Re}_\infty = \frac{dU}{\nu_\infty} = \frac{2rU}{\nu_\infty} \tag{8}$$

Throughout all the calculations the values of the Sherwood and Nusselt numbers utilized were those computed for the average conditions encountered at the surface of the sphere and the values of the Reynolds number were for the conditions in the free air stream.

In calculating values of the Sherwood and Nusselt numbers, an average temperature obtained by integration over the surface of the sphere was employed. The average surface temperature was determined from measurements of the local temperature as a function of polar angle by graphical solution of the following surface integral:

$$t_i^* = \frac{1}{A}\oint_0^A t_i\, dA \tag{9}$$

The variations in local surface temperatures were sufficient to result in a small added uncertainty in the evaluation of the macroscopic transport characteristics. As noted earlier, porous spheres, in contradistinction to drops (*15*), exhibit significant differences in temperature from point to point on the surface because of the lack of internal circulation and the variation in local material transport with position. It appeared satisfactory, nevertheless, to utilize Equation 9 to evaluate an average temperature and from this, average transport properties for the conditions at the interface.

In establishing the properties of the gas phase at the interface, it was assumed that the *n*-heptane and air form a binary ideal solution (*22*). Since the pressure was known, the composition of the gas phase at the interface could be predicted as a function of temperature, which varied from point to point around the sphere.

METHODS AND EQUIPMENT

The air supply equipment produced a stream with a velocity which could be varied from 4 to 32 feet per second. Details of the equipment are available (*12, 14*). The porous sphere, shown at A in Figure 1, was located at the exit of

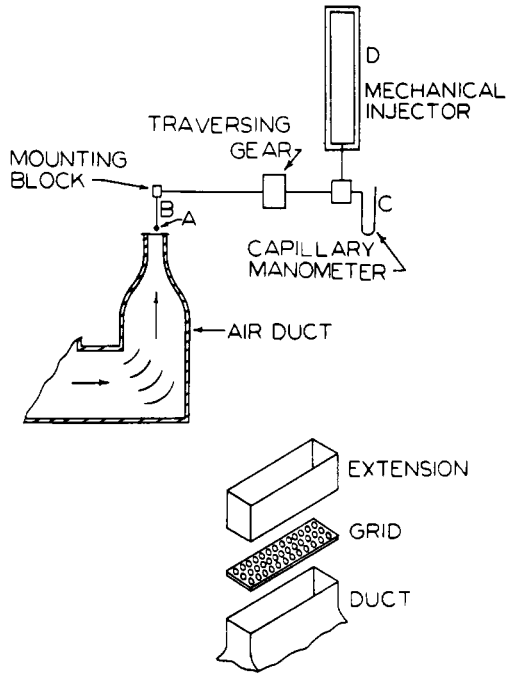

Figure 1. Arrangement of porous sphere

a duct, in a vertically emerging air jet approximately 3 by 12 inches.

The undisturbed air stream in the jet showed less than 2% variation in bulk velocity within 1 inch of the major axis of the jet. At velocities of 4 feet per second, the local fluctuations of temperature with time were as large as

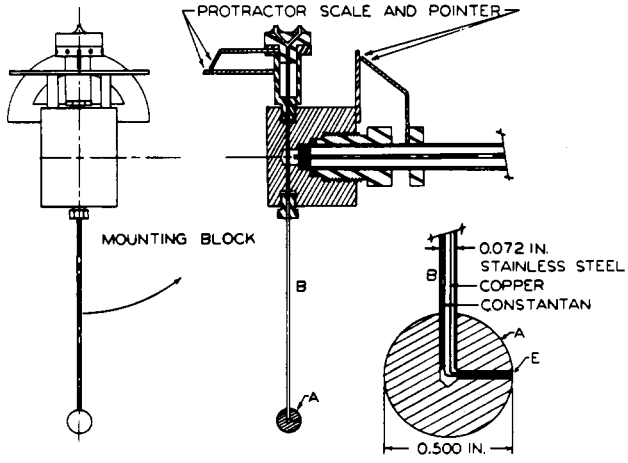

Figure 2. Details of porous sphere

0.09° F. However, at all the higher velocities these fluctuations were negligible. The average temperature of the stream was maintained within 0.05° F. of the chosen value. The average velocity of the stream was known with an uncertainty of 0.6%. The fractional transverse turbulence of the undisturbed stream was 0.013. This value was established from the data of Schubauer (*38*) used in conjunction with measurements of the divergence of the temperature profile in the wake of a heated wire.

The level of turbulence in the flowing stream was adjusted by placing the porous sphere at several different positions on the downstream side of a perforated plate, identical in design to one used by Davis (*5, 6*). Details of this grid, shown in a part of Figure 1, are available (*35*). Extensions, also illustrated in Figure 1, were provided in order to permit the stagnation point on the sphere to be located at nominal distances of 4, 6, 9, and 11 inches from the downstream face of the grid.

Significant variations in the average velocity were encountered with lateral position in the air stream at a distance of 3 inches from the downstream face of the grid. However, at greater distances these large scale variations were substantially eliminated. Variations in the longitudinal and transverse levels of turbulence with downstream distance from the grid were based upon the measurements of Davis (*6*) and are available (*35*). In relating the transverse turbulence level measured for the free jet with the longitudinal turbulence level in the wake of the perforated plate, it was assumed that the turbulence in the free jet was isotropic.

The porous sphere for the surface temperature measurements was prepared from a block of diatomaceous earth and was machined to a spherical contour within 0.0005 inch. A hole 0.072 inch in diameter was drilled to the center of the sphere, illustrated in Figure 2, and a thin-walled stainless steel tube, *B*, of approximately the same diameter was inserted. A capillary manometer, *C*, in Figure 1, approximately 0.01 inch in diameter was employed to measure the capillary pressure of the wetted porous sphere. A capillary pressure of approximately 40 p.s.i. was obtained. This pressure was highly sensitive to the position of the liquid interface near the surface of the sphere. A measure of the pressure at the center of the sphere thus afforded a convenient means of determining when the rate of introduction of *n*-heptane was just equal to the evaporation rate at the surface. This technique was similar to that employed by Schlinger (*36*).

As indicated in Figure 1 the supporting tube of the porous sphere was connected to a supply of *n*-heptane furnished by a mechanical injector, *D*, which determined the quantity of *n*-heptane introduced into the sphere within 0.1% (*12*). This made it possible to measure the rate of evaporation within 0.2% over the range of conditions encountered in this investigation. The attainment of steady state was indicated by the maintenance of a constant level in the capillary manometer, *C*, of Figure 1. It usually required a period of approximately 30 minutes to attain steady-state operation under a particular set of flow conditions.

The surface temperature of the sphere was determined by use of a copper-constantan thermocouple 0.003 inch in diameter set in the surface of the porous sphere, as indicated at *E* in Figure 2. The porous sphere could be rotated about the axis of the supporting tube, *B*, and rotation of the mounting block allowed angular motion of the sphere about a horizontal axis. This arrangement permitted the temperature of the surface to be determined as a function of polar angle, measured from the stagnation point.

For the second set of measurements, which included only measurements of the rate of evaporation of *n*-heptane, the same type of ceramic sphere was employed. It was mounted on a glass tube 0.03 inch in diameter, which was placed vertically in the air stream. Copper-constantan thermocouples, 0.003 inch in diameter, were located at the center of the sphere and in the glass tube at a distance of about 0.5 inch from the sphere. These thermocouples permitted the temperature at the center of the sphere to be determined and also made it possible to establish the temperature gradient in the glass tube. In the case of the evaporation measurements, the smaller glass tube was used in order to decrease the thermal conduction to the sphere. For the measurements of surface temperature, which involved introduction of the supporting tube at an angle to the flow, the use of a stiffer steel tube as described was necessary in order to avoid oscillation of the sphere.

All the thermocouples were calibrated in position against a platinum resistance thermometer of the coiled-filament type (*28*). The latter instrument had been compared with a reference instrument which was calibrated by the National Bureau of Standards. It is believed that the temperature of the thermocouple junctions was known within 0.05° F. relative to the international platinum scale. However, as a result of thermal conductivity along the thermocouple wires, uncertainty in the surface temperature of the sphere may have been as large as 0.2° F.

MATERIALS AND THEIR PROPERTIES

Values of the physical properties of air and *n*-heptane utilized in this study are available (*13*). The vapor pressure, enthalpy change upon vaporization, and specific gas constant for *n*-heptane were taken from the tabulations of Rossini (*33*). The isobaric heat capacity of *n*-heptane was taken from the data of Douglas (*7*) and the Maxwell diffusion coefficient for the molecular transport of *n*-heptane in the gas phase from the measurements by Schlinger (*36*). Uncertainties in the Maxwell diffusion coefficient probably are of the same order as the experimental uncertainties associated with the present investigation. The Benedict equation of state (*2*) was employed to establish the fugacity

Table I. Smoothed Values of Surface Temperature

Polar Angle, Degrees	Bulk Velocity, Ft./Sec. 4	8	16	32
	$\alpha_T = 0.013$			
0	62.6[a]	62.7	63.7	67.1
45	63.1	63.1	63.8	66.6
90	64.0	63.7	64.0	65.4
135	64.7	64.2	64.1	65.0
180	65.0	64.3	64.2	64.9
	$\alpha_T = 0.050$			
0	62.7	62.8	64.0	68.0
45	63.1	63.1	63.9	67.5
90	63.8	63.3	63.7	65.6
135	64.3	63.6	63.6	65.5
180	64.6	63.7	63.4	66.0
	$\alpha_T = 0.100$			
0	62.7	63.1	64.7	69.3
45	63.1	63.2	64.4	68.6
90	63.7	63.5	64.1	65.8
135	64.1	63.6	63.9	66.3
180	64.3	63.7	63.8	67.4
	$\alpha_T = 0.150$			
0	62.8	63.6	65.5	70.5
45	63.1	63.7	65.2	69.7
90	63.7	64.0	64.8	66.0
135	64.0	64.2	64.7	67.0
180	64.3	64.1	64.8	68.9

[a] Temperature in °F.

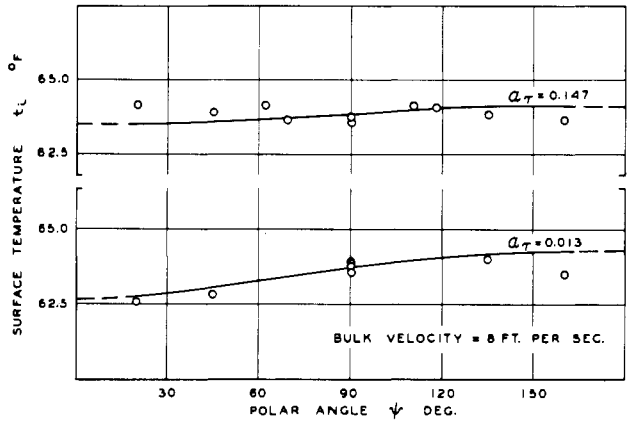

Figure 3. Experimental measurements of surface temperature

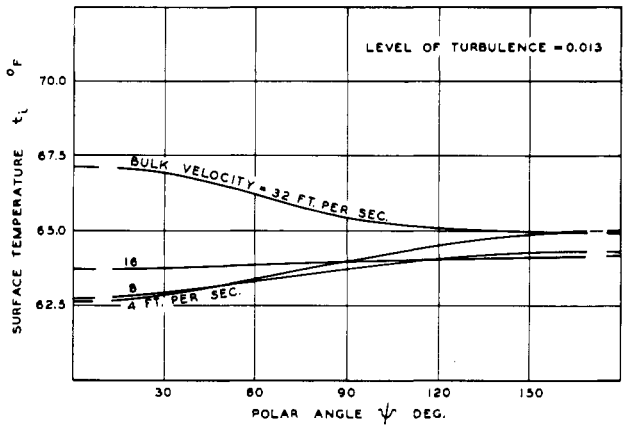

Figure 4. Variation in surface temperature in the free jet

of the *n*-heptane as a function of temperature and pressure. Thermal conductivity of the gas phase at the interface was established from information concerning the thermal conductivities of air (*30*) and *n*-heptane (*25*), by use of Hirschfelder's methods (*11*) for determining the transport properties of mixtures. The transport properties of the materials of construction of the sphere were obtained from the International Critical Tables (*18*). The *n*-heptane employed was obtained from the Phillips Petroleum Co. and was reported to contain less than 0.01 mole fraction of material other than *n*-heptane. It was further purified by fractionation in a glass column containing 16 plates at a pressure of approximately 7 p.s.i.a. and a reflux ratio of 40. The initial and final 10% portions of the overhead were discarded. The remainder of the overhead was passed as a liquid through a column of activated alumina 7 feet in length under ambient pressures and temperatures. The purified *n*-heptane had a specific weight of 42.429 pounds per cubic foot at 77° F., as compared with a value of 42.420 pounds per cubic foot reported by Rossini (*33*). The index of refraction was 1.3852 relative to the *D* lines of sodium at 77° F. as compared to a value of 1.38511 recorded by Rossini (*33*) for an air-saturated sample at the same temperature. To avoid the accumulation of impurities on the evaporating surface, the sphere was washed periodically with purified *n*-heptane.

EXPERIMENTAL RESULTS

The variation in surface temperature with polar angle and conditions of flow was investigated in some detail. Smoothed values of the surface temperature are presented in Table I as a function of polar angle taken from the stagnation point, of level of turbulence, and of bulk velocity. Detailed experimental data concerning the local surface temperatures are available (*3*). The standard deviation of all the smoothed data obtained from the experimental data was 0.37° F. It was computed from the expression:

$$\sigma = \left[\frac{\Sigma (t_{i\,\mathrm{exp}} - t_{i\,\mathrm{sm}})^2}{N-1}\right]^{1/2} \qquad (10)$$

Relative values of this measure of uncertainty were defined as the quotient of the standard deviation and the difference between the free stream temperature and the average experimental surface temperature. The average value of this quantity for all the measurements was found to be 0.006. A detailed analysis of the deviations of the experimental from smoothed data is available (*3*). Figure 3 shows a representative sample of the experimental measurements of surface temperature as a function of polar angle measured from the stagnation point. These data are presented for a bulk velocity of 8 feet per second and include surface temperatures for two levels of turbulence. The curves are from the smoothed data of Table I and obviously are not in detailed agreement with the limited number of points presented in Figure 3 but represent the best fit to all of the surface temperature data available (*3*).

To illustrate the smoothed data from Table I, Figure 4 shows the variation in surface temperature with polar angle measured from the stagnation point for the free jet. The marked influence of bulk velocity is of interest. The influence of level of turbulence upon the temperature distribution for a velocity of 32 feet per second is depicted in Figure 5. The effect of level of turbulence is less pro-

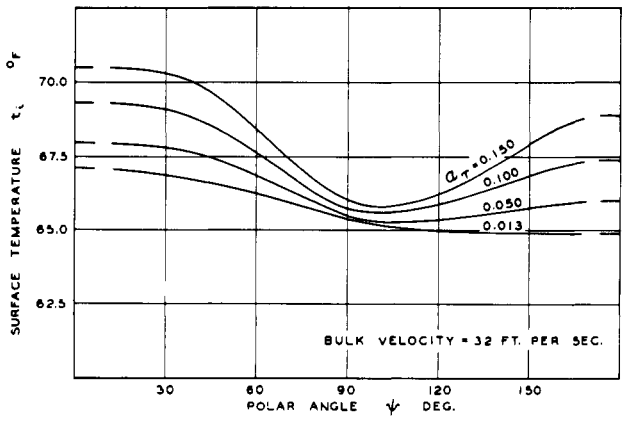

Figure 5. Influence of level of turbulence on local surface temperature

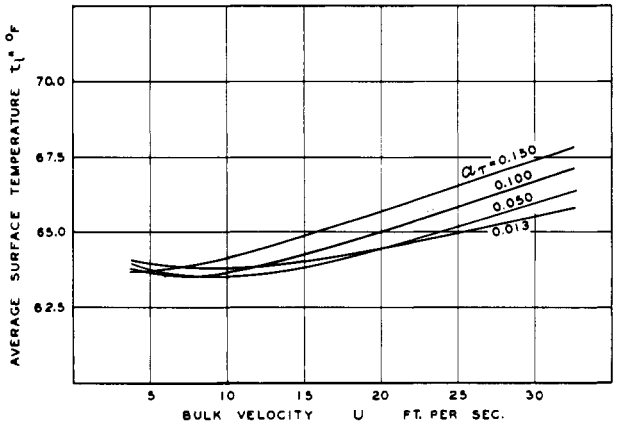

Figure 6. Influence of level of turbulence on average surface temperature

nounced at lower velocities as shown in Figure 3. Under natural convective conditions significant, nearly random variations in the surface temperature with time were experienced. Moreover, an average surface temperature of approximately 57.6° F. was found for natural convection. This value differs markedly from those shown in Table I or in Figures 4 or 5. Such a difference may result from a reversal in the direction of flow about the sphere under natural convection, as a result of the specific volume of the

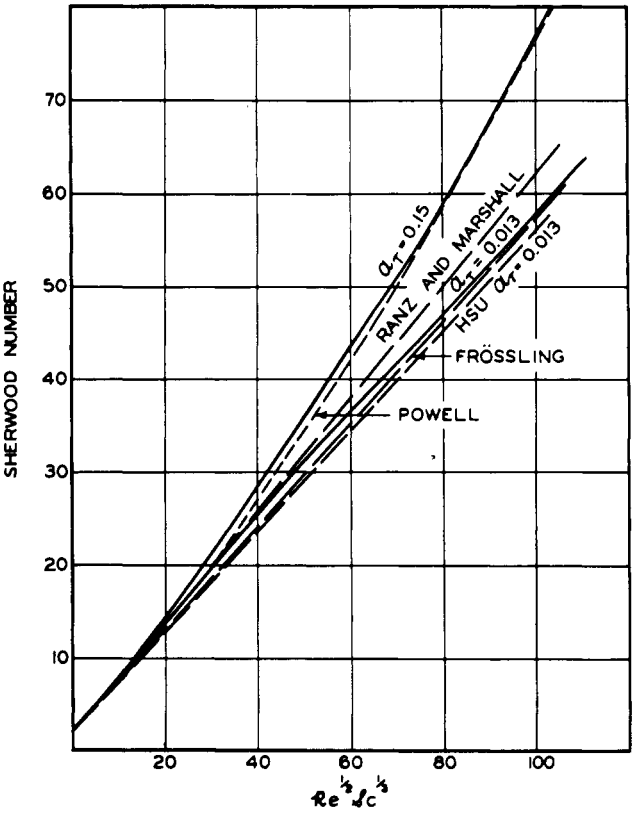

Figure 7. Effect of Reynolds number on Sherwood number

gases being lower in the boundary region than in the main body of the stream.

The magnitude of the variations in temperature from point to point on the sphere is sufficient to make difficult any interpretation of an average surface temperature. Table II records, nevertheless, average surface temperatures obtained by application of Equation 9. Figure 6 shows the influence of level of turbulence and velocity upon the average surface temperature. It is apparent that conditions of flow have little influence on the average surface temperature. The level of turbulence appears to have nearly as great an effect as the velocity.

Table II includes experimental information associated with the evaporation of *n*-heptane. The data are divided into five parts. The first pertains to behavior in the undisturbed free jet and the other four parts to nominal distances of 4, 6, 9, and 11 inches downstream of the aft face of the perforated plate. The information submitted in Table II comprises, in addition to the average temperature at the surface of the sphere as established from Table I, the fugacity of *n*-heptane, the weight rate of evaporation, the level of turbulence, the bulk velocity, and other information concerning the experimental measurements. In a few instances two or more sets of values for a given set of conditions are included. The Reynolds number for free stream conditions, the heat transfer coefficient, and the values of the Sherwood and Nusselt numbers for surface conditions, computed by application of Equations 6 and 3, respectively, are recorded in Table III for each set of conditions presented in Table II.

By utilizing information from Tables II and III, the influence of Reynolds number upon the Sherwood and Nusselt numbers for a constant level of turbulence was evaluated. Table IV records values of the Sherwood and Nusselt numbers for the sphere for a variety of conditions of flow. Values of the Nusselt number both corrected and uncorrected for radiant transport from the sphere are presented. It was necessary to utilize an iterative smoothing operation, because the experimental data were not obtained at even values of the level of turbulence or of the Reynolds number. The standard deviation of the Sherwood number was 2.0 and of the uncorrected Nusselt number 2.2, assuming that all the error lay in the material and thermal transfer and none in the conditions of flow. A detailed consideration of the agreement of the experimental and smoothed data is available (*3*).

Figure 7 illustrates the effect of the Reynolds number on the Sherwood number for two levels of turbulence. The data of Ranz and Marshall (*32*), Frössling (*9*), Powell (*31*), and Hsu (*14*) are included for comparison. In accordance with the analysis of Frössling (*9*), the variable $Re^{1/2} Sc^{1/3}$ was used as the independent variable, in order to obtain a more nearly linear variation of the Sherwood number with conditions of flow. It was not possible to show the experimental points obtained in the present investigation because there was a simultaneous variation in the Reynolds number and in

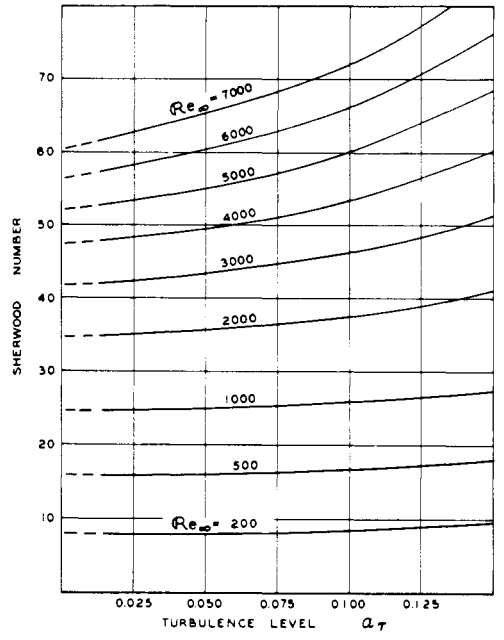

Figure 8. Variation in Sherwood number with level of turbulence

the level of turbulence for all of the experimental work undertaken. It is apparent that the data of Frössling (*9*) agree well with the current measurements for a zero level of turbulence, whereas the measurements of Ranz and Marshall (*32*) appear to correspond with the present measurements at an intermediate level of turbulence. The data of Hsu (*14*) for spherical drops are also in good agreement with the present data. Powell's measurements (*31*) indicate a larger rate of transport than would be expected for the level of turbulence estimated from the arrangement of his air supply.

Figure 8 presents the variation in the Sherwood number with level of turbulence, using the Reynolds number as a parameter. The figure shows a marked increase in the Sherwood number with an increase in the level of turbulence

Table II. Experimental Data for Evaporation of *n*-Heptane

Test No.	Pressure, P.S.I.A.	Air Temp., °F.	Weight Fraction Water in Air	Bulk Velocity, Ft./Sec.	Distance Downstream from Grid, Inches	Turbulence Level Fraction	Mole Fraction Moist Air[a]	Fugacity of *n*-Heptane, Lb./Sq.Ft. Gas	Fugacity of *n*-Heptane, Lb./Sq.Ft. Liquid	Maxwell Diffusion Coefficient, Lb./Sec.	Av Surface Temp.[b] °F.	Total Evaporation, Lb./Sec. ($\times 10^{-6}$)	Total Thermal Transfer, B.t.u./Sec. ($\times 10^{-3}$)
45	14.226	99.9	0.0074	3.68	No grid	0.013	0.94882	1812.92	92.79	0.15689	64.11	2.494	0.3164
48	14.348	100.1	0.0060	3.65	No grid	0.013	0.94930	1826.67	92.79	0.15689	64.11	2.721	0.3531
50	14.270	100.2	0.0057	3.97	No grid	0.013	0.94904	1817.83	92.64	0.15686	64.08	2.720	0.3512
165	14.324	100.0	0.0076	4.06	No grid	0.013	0.94914	1818.83	92.50	0.15686	64.06	2.528	0.3188
201-A	14.359	100.0	0.0100	4.04	No grid	0.013	0.94898	1827.81	93.36	0.15685	64.05	2.708	0.3279
												2.820	0.3335
46	14.245	99.6	0.0069	8.06	No grid	0.013	0.94942	1814.69	91.79	0.15668	63.76	3.777	0.4968
												3.710	0.4974
49	14.339	100.2	0.0071	7.82	No grid	0.013	0.94970	1825.24	91.79	0.15668	63.77	3.795	0.4968
52	14.332	100.1	0.0074	8.04	No grid	0.013	0.94966	1823.34	91.79	0.15668	63.76	3.807	0.5001
201-B	14.390	100.0	0.0078	7.83	No grid	0.013	0.94924	1830.92	92.93	0.15668	63.77	3.671	0.4514
												3.768	0.4649
												3.929	0.4873
198	14.377	100.1	0.0081	16.20	No grid	0.013	0.94887	1831.70	93.65	0.15689	64.12	4.807	0.6108
												4.964	0.6326
												5.281	0.6770
200	14.330	100.0	0.0079	16.28	No grid	0.013	0.94868	1824.65	93.65	0.15689	64.12	4.985	0.6312
												4.987	0.6315
												5.338	0.6805
47	14.300	100.1	0.0067	20.50	No grid	0.013	0.94933	1822.45	92.35	0.15738	64.98	5.850	0.7907
51	14.368	100.1	0.0056	20.39	No grid	0.013	0.94956	1830.99	92.35	0.15737	64.97	6.049	0.8142
												6.037	0.8126
199	14.335	100.2	0.0090	32.24	No grid	0.013	0.94658	1827.64	97.64	0.15784	65.78	7.261	0.9546
104-B	14.372	100.1	0.0068	4.06	12.04	0.058	0.94966	1829.19	92.07	0.15675	63.88	2.761	0.3524
					11.04	0.062	0.94964	1829.13	92.07	0.15673	63.85	2.781	0.3545
					10.04	0.068	0.94974	1829.11	91.93	0.15673	63.83	2.789	0.3555
104-C	14.382	100.1	0.0058	8.03	12.03	0.058	0.95014	1829.59	91.22	0.15654	63.52	3.911	0.5100
					11.03	0.063	0.95014	1829.57	91.22	0.15654	63.51	3.937	0.5134
					10.03	0.068	0.95014	1829.57	91.22	0.15654	63.51	3.942	0.5140
107	14.449	100.1	0.0065	8.04	13.04	0.056	0.95004	1825.93	91.22	0.15654	63.52	3.888	0.5068
104-A	14.395	100.1	0.0063	16.15	12.04	0.055	0.94973	1831.58	92.07	0.15675	63.89	5.564	0.7408
					11.04	0.059	0.94965	1831.64	92.22	0.15678	63.91	5.604	0.7463
					10.04	0.064	0.94966	1831.70	92.22	0.15679	63.95	5.624	0.7493
108	14.308	100.1	0.0061	16.23	13.03	0.952	0.94933	1819.85	92.22	0.15675	63.88	5.515	0.7325
	14.323	100.1	0.0063	4.05	9.01	0.075	0.94959	1823.51	91.93	0.15671	63.81	2.785	0.3550
					8.01	0.083	0.94958	1823.47	91.93	0.15670	63.79	2.802	0.3569
					7.01	0.093	0.94958	1823.47	91.93	0.15670	63.78	2.823	0.3595
106-C	14.331	100.1	0.0091	4.04	10.11	0.071	0.94890	1824.38	93.22	0.15673	63.85	2.736	0.3123
												2.856	0.3380
207-A	14.349	100.1	0.0055	8.03	9.01	0.075	0.95004	1825.89	91.22	0.15635	63.50	3.951	0.5155
					8.01	0.083	0.95004	1825.89	91.22	0.15653	63.50	4.000	0.5221
					7.01	0.093	0.94997	1825.95	91.36	0.15656	63.55	4.035	0.5263
106-B	14.337	100.1	0.0100	8.10	10.11	0.070	0.94951	1829.58	92.22	0.15650	63.45	3.917	0.4855
												4.072	0.5072
207-B	14.301	100.1	0.0060	16.21	9.01	0.071	0.94929	1821.34	92.36	0.15682	64.00	5.654	0.7530
					8.01	0.078	0.94914	1821.38	92.36	0.15686	64.08	5.719	0.7624
					7.01	0.087	0.94906	1821.40	92.64	0.15690	64.14	5.796	0.7724
106-A	14.375	100.1	0.0098	16.16	10.12	0.065	0.94904	1829.38	93.22	0.15677	63.91	5.389	0.6908
												5.612	0.7220
												5.745	0.7405
208	14.326	100.2	0.0077	32.21	10.06	0.060	0.94571	1827.48	99.21	0.15821	66.42	7.840	1.0435
												8.137	1.0852
209	14.312	100.1	0.0065	4.07	6.06	0.106	0.94963	1822.23	91.79	0.15667	63.75	2.883	0.3670
105-B					5.06	0.123	0.94971	1822.19	91.64	0.15666	63.72	2.914	0.3722
					4.06	0.146	0.94971	1822.17	91.64	0.15666	63.71	3.051	0.3881
206-A	14.321	99.8	0.0083	4.07	7.16	0.094	0.94903	1823.06	92.93	0.15667	63.74	2.767	0.3230
												2.839	0.3330
												2.904	0.3426
98	14.307	100.1	0.0107	8.08	7.07	0.094	0.94983	1821.16	91.36	0.15656	63.55	3.931	0.5137
105-A	14.326	100.1	0.0060	8.05	6.06	0.106	0.94982	1823.41	91.50	0.15659	63.61	4.056	0.5291
					5.06	0.123	0.94975	1823.62	91.64	0.15666	63.72	4.232	0.5257
					4.06	0.146	0.94944	1823.89	92.22	0.15658	63.92	4.483	0.4881
206-B	14.346	99.8	0.0091	8.04	7.16	0.092	0.94926	1825.98	92.65	0.15655	63.53	3.802	0.4667
												3.905	0.4809
99	14.305	100.1	0.0057	16.22	7.07	0.088	0.94906	1821.59	92.79	0.15690	64.15	5.681	0.7552
105-C	14.314	100.1	0.0058	16.22	6.06	0.097	0.94893	1823.17	93.22	0.15689	64.29	5.890	0.7848
					5.06	0.111	0.94943	1823.38	92.21	0.15709	64.47	6.179	0.8259
					4.06	0.130	0.94834	1823.69	94.22	0.15724	64.73	6.631	0.8888
205	14.397	100.8	0.0077	16.11	7.18	0.087	0.94889	1832.25	93.65	0.15690	64.14	5.448	0.6972
												5.534	0.7093
210	14.323	100.0	0.0120	32.22	7.18	0.078	0.94540	1827.55	99.78	0.15838	66.71	8.000	1.0625
												8.237	1.0959
203-A	14.367	100.9	0.0091	4.10	4.21	0.151	0.94917	1828.20	92.93	0.15666	63.72	2.887	0.3426
												2.950	0.3514
												3.045	0.3647
101	14.346	100.1	0.0060	8.03	4.09	0.148	0.94950	1826.23	92.22	0.15679	63.94	4.731	0.6267
203-B	14.289	100.9	0.0100	8.07	4.21	0.147	0.94870	1819.84	93.36	0.15680	63.96	4.142	0.5175
												4.491	0.5656
100	14.417	100.1	0.0052	16.22	4.09	0.135	0.94990	1834.98	91.93	0.15728	64.80	6.467	0.8650
103	14.286	100.1	0.0058	16.25	6.06	0.097	0.94878	1820.01	93.22	0.15698	64.29	5.875	0.7839
					5.06	0.111	0.94935	1820.50	92.22	0.15709	64.47	6.171	0.8257
204-A	14.301	100.8	0.0098	16.26	4.20	0.143	0.94746	1822.50	95.79	0.15735	64.93	6.114	0.7941
												6.220	0.8090
												6.354	0.8278
204-B	14.417	100.8	0.0077	31.98	4.20	0.116	0.94496	1838.92	101.21	0.15869	67.25	9.497	1.2763
												9.631	1.2952

[a] Composition at interface.
[b] See Equation 9.

Table III. Nusselt and Sherwood Numbers

Test No.	Reynolds No., Free Stream	Heat Transfer Coefficient, B.t.u./(Sec.)(Sq.Ft.)(°F.) ($\times 10^{-3}$)	Sherwood No. Surface	Nusselt Number Surface	
				Corr.	Uncor.[a]
45	822	1.621	21.45	16.77	18.40
48	823	1.799	23.97	18.61	20.18
50	889	1.834	23.94	18.97	20.65
165	907	1.626	22.20	16.82	18.64
201-A	911	1.674	23.74	17.32	19.02
		1.703	24.72	17.62	19.32
46	1802	2.542	33.58	26.29	27.96
		2.545	32.99	26.32	27.46
409	1760	2.500	33.75	25.87	27.54
52	1807	2.522	33.87	26.10	27.75
201-B	1768	2.287	32.32	23.66	25.37
		2.355	33.18	24.37	26.08
		2.469	34.59	25.55	27.15
198	3657	3.119	41.99	32.26	33.95
		3.230	43.36	33.40	35.09
		3.457	46.14	35.75	37.45
200	3662	3.228	43.50	33.38	35.33
		3.230	43.55	33.40	35.34
		3.480	46.59	35.99	37.93
47	4602	4.128	51.61	42.64	44.50
51	4599	4.249	53.40	43.88	45.57
		4.241	53.29	43.79	45.49
199	7251	5.088	60.67	52.54	54.52
104-B	911	1.784	24.48	18.45	20.17
		1.793	24.65	18.55	20.27
		1.797	24.77	18.59	20.53
104-C	1813	2.628	35.04	27.19	28.99
		2.645	35.27	27.37	29.17
		2.648	35.32	26.40	29.20
107	1811	2.540	34.82	26.29	28.26
104-A	3649	3.751	49.34	38.81	40.50
		3.781	49.61	39.11	41.00
		3.800	49.79	39.30	41.00
108	3649	3.711	48.62	38.39	40.16
106-C	912	1.794	24.99	18.56	20.27
		1.802	24.87	18.64	20.37
		1.815	25.06	18.77	20.50
207-A	909	1.584	24.00	16.39	18.57
		1.715	25.05	17.74	19.45
106-B	1803	2.582	35.38	26.72	28.44
		2.615	35.83	27.06	28.78
		2.640	36.08	27.32	29.03
207-B	1823	2.436	34.76	25.22	26.89
		2.545	36.14	26.35	28.02
106-A	3642	3.824	49.94	39.55	40.91
		3.881	50.36	40.14	41.88
		3.938	50.95	40.74	42.47
208	3747	3.511	47.27	36.33	38.05
		3.669	49.23	37.96	39.69
		3.763	50.40	38.94	40.66
209	7240	5.684	64.24	58.64	60.34
		5.911	66.67	60.98	62.68
105-B	914	1.851	25.74	19.15	20.92
		1.876	26.06	19.41	21.18
		1.955	27.28	20.23	22.01
206-A	916	1.643	24.36	17.00	18.85
		1.694	24.99	17.53	19.37
		1.743	25.60	18.04	19.88
98	1815	2.576	35.14	26.65	28.37
105-A	1810	2.659	36.20	27.51	29.26
		2.649	37.71	27.41	29.17
		2.474	39.73	25.59	27.34
206-B	1812	2.361	33.58	24.44	26.28
		2.432	34.49	25.17	27.02
99	3642	3.852	49.93	39.84	41.67
105-C	3645	4.018	51.61	41.55	43.35
		4.250	54.64	43.93	45.72
		4.607	57.33	47.62	49.41
205	3634	3.635	47.56	36.08	37.90
		3.698	48.31	36.71	38.53
210	7244	5.718	65.12	58.99	60.92
		5.897	67.06	60.83	62.76
203-A	922	1.692	25.41	17.51	19.14
		1.735	25.97	17.95	19.59
		1.801	32.07	18.63	20.27
101	1808	3.270	41.88	33.82	34.87
203-B	1806	2.572	36.20	26.61	28.27
		2.811	39.25	29.08	30.77
100	3671	4.493	57.24	46.43	48.29
103	3644	4.014	51.39	41.51	43.46
		4.249	54.55	43.92	45.46
204-A	3642	4.061	52.08	41.98	43.78
		4.138	52.98	42.77	44.56
204-B	7222	6.979	76.66	71.94	73.84
		7.082	77.74	73.00	74.91

[a] Uncorrected for radiant transport.

for fixed values of the higher Reynolds numbers. The Sherwood numbers in Figures 7 and 8 were based upon the transport properties of the gas phase for the temperature and composition at the interface.

To illustrate in greater detail the influence of level of turbulence upon material transport from spheres, the relative Sherwood number as a function of level of turbulence is shown in Figure 9. The relative Sherwood number was defined as the ratio of the Sherwood number at a given level of turbulence to the Sherwood number for nonturbulent flow. It is apparent that at the higher Reynolds numbers the influence of the level of turbulence is pronounced and may increase the material transport nearly 40% at a level of turbulence of 0.15.

For the sake of comparison, the data of Maisel and Sherwood (27) are shown in terms of the relative Sherwood number in Figure 10. These data are presented as a function of the reported level of turbulence. For the convenience of the reader, the present measurements have been interpolated to Reynolds numbers similar to those employed by Maisel and Sherwood. It is seen from the figure that Maisel's measurements were made at two scales of turbulence resulting from the two sizes of perforation in the plate used to induce turbulence. It does not appear that this change in scale of turbulence influenced his results greatly. The present data indicate a somewhat greater

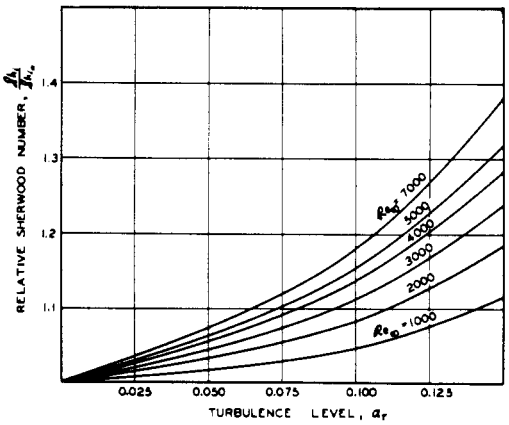

Figure 9. Relative Sherwood number as a function of level of turbulence

effect of level of turbulence upon transport rate than do the data of Maisel and Sherwood. For the present study data of Davis (6) were used to relate position in the wake of the plate to turbulence level, whereas Maisel and Sherwood made these measurements directly. Differences in the method of measurement of the level of turbulence may

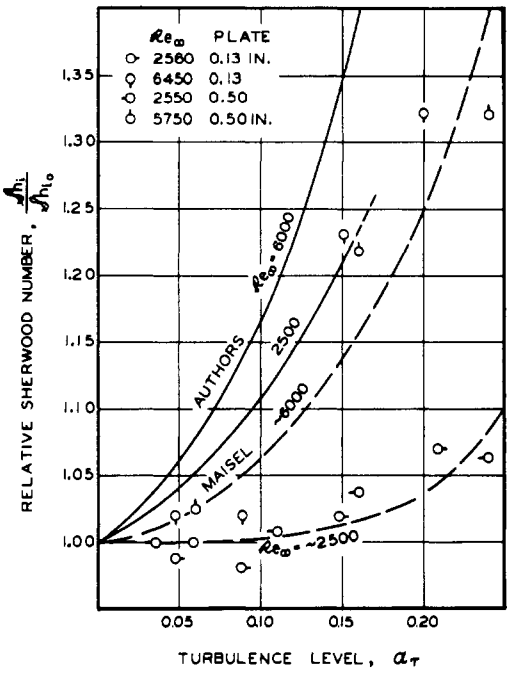

Figure 10. Comparison of results from two investigations

account for some of the difference between the two sets of data.

The values of the Nusselt number for the associated convective thermal transport, as corrected for radiant transport, are presented as a function of Reynolds number for two levels of turbulence in Figure 11. The recommended values from McAdams (*25*) together with the measurements of Kramers (*20*), Sato (*35*) for spheres, and Hsu (*14*) for spherical drops are included. For the most part the current data support the results obtained by Sato and Hsu and are in fair agreement with the measurements of Kramers, when considering that turbulence level was not reported in his work. It appears from a consideration of the present measurements that the values recommended by McAdams are high, even for fully developed turbulent shear flow, and that radiant energy transport may not have been taken into account. In Figure 12 the Nusselt number for varying levels of turbulence as determined for a silver sphere (*35*), for which only thermal transport is involved, is compared with some of the present results. Good agreement is obtained at low level of turbulence. These data indicate similar trends in the influence of the level of turbulence upon the Nusselt number for thermal transport and for combined material and thermal transport.

To illustrate the comparative effect of level of turbulence

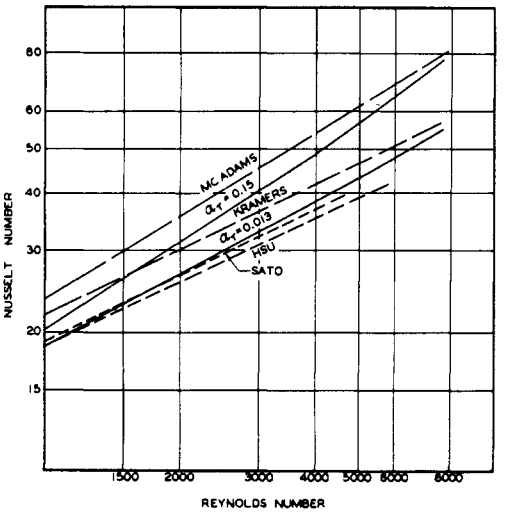

Figure 11. Nusselt number as a function of Reynolds number

Table IV. Sherwood and Nusselt Numbers for Material Transport from Spheres

Reynolds No.	Sherwood No.	Nusselt No. Corrected	Nusselt No. Uncorrected[a]	Sherwood No.	Nusselt No. Corrected	Nusselt No. Uncorrected[a]
		$\alpha_T = 0.00$[b]			$\alpha_T = 0.100$	
1000	24.8	18.6	20.6	26.0	18.8	21.1
2000	34.9	26.3	28.4	37.6	28.2	30.5
3000	42.0	32.4	34.5	46.4	35.8	38.0
4000	47.7	37.9	39.9	53.5	42.8	44.9
5000	52.2	42.4	44.9	60.2	49.5	51.5
6000	56.6	47.1	49.2	66.0	55.5	57.7
7000	60.6	51.3	53.4	71.9	61.1	63.2
		$\alpha_T = 0.013$			$\alpha_T = 0.150$	
1000	24.9	18.6	20.7	27.6	20.2	22.4
2000	35.1	26.5	28.8	41.2	31.2	33.5
3000	40.3	32.8	35.0	51.4	40.1	42.1
4000	47.9	38.2	40.2	60.2[b]	48.0[b]	50.1[b]
5000	52.8	43.0	45.7	68.4[b]	56.7[b]	58.6[b]
6000	57.5	47.8	50.2	76.0[b]	64.4[b]	66.4[b]
7000	61.6	52.2	54.8	83.8[b]	72.1[b]	74.0[b]
		$\alpha_T = 0.050$				
1000	25.1	18.7	20.8			
2000	35.9	27.0	29.3			
3000	43.5	33.8	36.0			
4000	49.7	39.6	41.5			
5000	55.3	45.1	47.3			
6000	60.6	50.5	52.7			
7000	65.5	55.5	57.7			

[a]Uncorrected for radiant transport.
[b]Extrapolated.

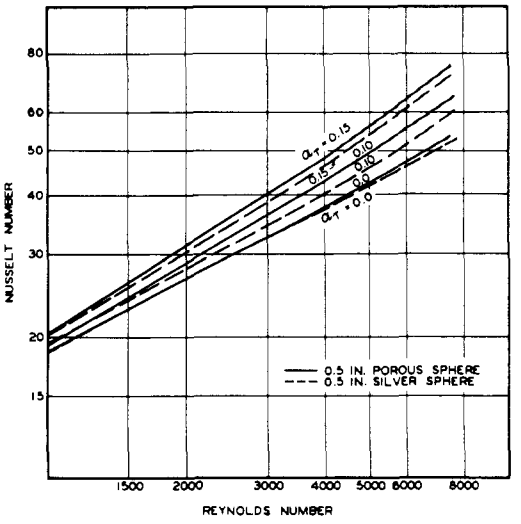

Figure 12. Nusselt number for porous sphere and silver sphere

upon material and thermal transport, Figure 13 shows the relative Nusselt number for transport from a silver sphere (*35*) and the relative Nusselt and Sherwood numbers for transport from a porous sphere. The relative Nusselt number has a definition similar to that given earlier for the relative Sherwood number. The data are presented for a Reynolds number of 5000. The difference in the two curves for Nusselt number is an indication of the effect of material flux upon the boundary flows.

ACKNOWLEDGMENT

The Fluor Corp. contributed to support of the experimental program. N. T. Hsu, a Peter E. Fluor fellow, assisted with some of the experimental measurements. The assistance of Lorine Faris and Virginia Berry in connection with the preparation of the data in a form suitable for publication is acknowledged. Ann Hansen assembled the manuscript, which was reviewed by W. N. Lacey.

NOMENCLATURE

A = area, sq. feet
b = specific gas constant, feet per °R.
C_p = isobaric heat capacity, B.t.u./(lb.) (°F.)
$D_{F,k}$ = Fick diffusion coefficient of component k, sq.foot/sec.
$D_{M,k}$ = Maxwell diffusion coefficient of component k, lb./sec.
d = differential operator
d = diameter of sphere, inches or feet
f_k° = fugacity of component k, pure state, lb./sq.foot
H = enthalpy, B.t.u./lb.
h = heat transfer coefficient, B.t.u./(sec.)(sq.ft.)(°F.)
K = constant of proportionality
k = thermal conductivity, B.t.u./(sec.)(sq.ft.)(°F./ft.)
L = latent heat of vaporization, B.t.u./lb.
l = characteristic length, inches or feet
$\dot{m}$ = evaporation rate, lb./(sec.)(sq.ft.)
$\dot{\underline{m}}$ = total material transfer rate from the surface, pounds per second
m_c = material transfer coefficient, feet per second
N = number of experimental points
n = radial distance in a direction normal to axis
n = mole fraction
Nu = Nusselt number
P = pressure, lb./sq.ft.
Pr = Prandtl number
$\dot{Q}$ = local thermal flux from the surface, B.t.u./(sec.)(sq.ft.)
$\dot{\underline{Q}}$ = total thermal transfer rate from the surface, B.t.u./sec.
$\dot{\underline{Q}}_r$ = total radiant transport rate from the surface, B.t.u./sec.
$\dot{\underline{Q}}_t$ = total conduction from sphere through tube and its contents, B.t.u./sec.
r = radius, inches or feet
Re = Reynolds number
Sc = Schmidt number $\dfrac{\nu_\infty}{D_{F,k}} \approx \dfrac{P\nu_\infty}{D_{M,k}}$

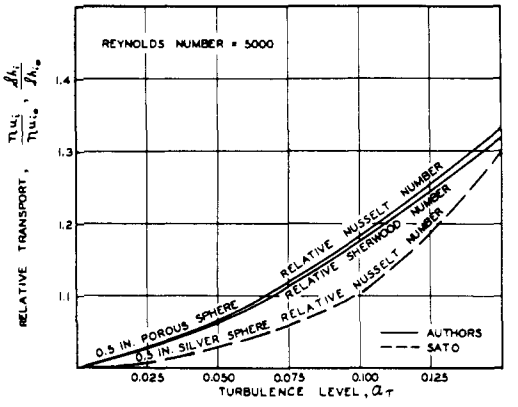

Figure 13. Relative Nusselt and Sherwood numbers

Sh = Sherwood number
T = thermodynamic temperature, °R.
t = temperature, °F.
U = bulk velocity, feet per second
x = distance along coordinate axis, feet
Z = compressibility factor
α_T = longitudinal turbulence level
β = Stefan-Boltzmann constant = 0.04758×10^{-11}, B.t.u./(sec.)(sq.ft.)(°R.)^4
ϵ = emissivity
ν = kinematic viscosity, sq.ft./sec.
σ = standard deviation
$\phi(\ )$ = function of
ψ = polar angle measured from the stagnation point, degrees

Subscripts

exp = experimental
g = gas phase
i = gas-liquid interface
j = air
k = n-heptane
l = liquid phase
0 = zero level of turbulence
sm = smoothed
sp = sphere
sr = surroundings
t = supporting tube
w = thermocouple wire
∞ = free stream

Superscripts

α = exponent
$*$ = space average

LITERATURE CITED

(1) Bedingfield, C. H., Jr., Drew, T. B., *Ind. Eng. Chem.* **42**, 1164-73 (1950).
(2) Benedict, M., Webb, G. B., Rubin, L. C., *Chem. Eng. Progr.* **47**, 449-54 (1951).
(3) Brown, R. A. S., Sato, K., Sage, B. H., *Am. Doc. Inst.*, Washington 25, D. C., Document 5600 (1958).

(4) Comings, E. W., Clapp, J. T., Taylor, J. F., *Ind. Eng. Chem.* **40**, 1076–82 (1948).
(5) Davis, L., Jet Propulsion Lab., Pasadena, Calif., Rept. 3–22, 1950.
(6) *Ibid.*, 3–17, 1952.
(7) Douglas, T. B., Furukawa, G. T., Coskey, R. E., Ball, A. F., *J. Research Natl. Bur. Standards.* **53**, 139–53 (1954).
(8) Frössling, N., *Gerlands Beitr. Geophys.* **51**, 167–73 (1937).
(9) *Ibid.*, **52**, 170–216 (1938).
(10) Groot, S. R. de, "Thermodynamics of Irreversible Processes," Interscience, New York, 1952.
(11) Hirschfelder, J. O., Curtiss, C. F., Bird, R. B., "Molecular Theory of Gases and Liquids," Wiley, New York, 1954.
(12) Hsu, N. T., Reamer, H. H., Sage, B. H., *Am. Doc. Inst.*, Washington 25, D. C., Document 4219 (1954).
(13) Hsu, N. T., Sage, B. H., *Ibid.*, Document 5311 (1957).
(14) Hsu, N. T., Sato, K., Sage, B. H., *Ind. Eng. Chem.* **46**, 870–76 (1954).
(15) Hughes, R. R., Gilliland, E. R., *Chem. Eng. Progr.* **48**, 497–504 (1952).
(16) Ingebo, R. D., Natl. Advisory Comm. Aeronaut., Tech. Note 2368 (1951).
(17) *Ibid.*, Tech. Note 2850 (1953).
(18) International Critical Tables, vol. 5, McGraw-Hill, New York, 1929.
(19) Kirkwood, J. G., Crawford, B., Jr., *J. Phys. Chem.* **56**, 1048–51 (1952).
(20) Kramers, H., *Physica* **12**, 61–80 (1946).
(21) Langmuir, I., *Phys. Revs.* **12**, 368–70 (1918).
(22) Lewis, G. N., *J. Am. Chem. Soc.* **30**, 668–83 (1908).
(23) Lewis, G. N., *Proc. Am. Acad. Arts Sci.* **37**, 49–69 (1901).
(24) Linton, W. H., Jr., Sherwood, T. K., *Chem. Eng. Progr.* **46**, 258–64 (1950).
(25) McAdams, W. H., "Heat Transmission," 3rd ed., McGraw-Hill, New York, 1954.
(26) Maisel, D. S., Sherwood, T. K., *Chem. Eng. Progr.* **46**, 131–88 (1950).
(27) *Ibid.* **46**, 172–5 (1950).
(28) Meyers, C. H., *Bur. Standards J. Research* **9**, 807–13 (1932).
(29) Morse, H. W., *Proc. Am. Acad. Arts Sci.* **45**, 361–7 (1910).
(30) Page, F., Jr., Corcoran, W. H., Schlinger, W. G., Sage, B. H., Am. Doc. Inst., Washington 25, D. C., Document 3293 (1952).
(31) Powell, R. W., *Trans. Inst. Chem. Engrs. (London)* **18**, 36–50 (1940).
(32) Ranz, W. E., Marshall, W. R., Jr., *Chem. Eng. Progr.* **48**, 141–6, 173–80 (1952).
(33) Rossini, F. D., others, "Selected Values of Physical and Thermodynamic Properties of Hydrocarbons and Related Compounds," Carnegie Press, Pittsburgh, 1953.
(34) Sage, B. H., *Chem. Eng. Progr.* **49**, Letter to Editor (July 1953).
(35) Sato, K., Sage, B. H., "Thermal Transfer in Turbulent Gas Streams. Effect of Turbulence on Macroscopic Transport from Spheres," Paper 57-A-20, Heat Transfer Division, Annual Meeting, New York, N. Y., December 1957, Am. Soc. Mech. Engrs.
(36) Schlinger, W. G., Reamer, H. H., Sage, B. H., Lacey, W. N., "Report of Progress-Fundamental Research on Occurrence and Recovery of Petroleum, 1952–1953," Am. Petroleum Inst., pp. 70–106.
(37) Schlinger, W. G., Sage, B. H., Am. Doc. Inst., Washington 25, D. C., Document 4221 (1954).
(38) Schubauer, G. B., Natl. Advisory Comm. Aeronaut., Rept. 524 (1935).

Received for review July 1, 1957. Accepted December 20, 1957. Material supplementary to this article has been deposited as Document No. 5600 with the ADI Auxiliary Publications Project, Photoduplication Service, Library of Congress, Washington 25, D. C. A copy may be secured by citing the document number and by remitting $2.50 for photoprints or $1.75 for 35-mm. microfilm. Advance payment is required. Make checks or money orders payable to Chief, Photoduplication Service, Library of Congress.

Specific Heats of Aviation Hydraulic Fluids

ROGER S. PORTER and JULIAN F. JOHNSON
California Research Corp., Richmond, Calif.

It is useful to know the specific heats of hydraulic fluids over wide temperature ranges. For the severe conditions under which such fluids perform in modern supersonic aircraft, specific heat is quantitatively considered in heat transfer calculations in aircraft design. It is instrumental in determining rates of heating or cooling under unsteady state conditions. The choice of a hydraulic fluid with a given specific heat will thus influence the transient thermal response characteristics of the hydraulic system and will partially define its thermal performance.

Empirical correlations have proved very satisfactory for predicting the specific heats of the common pure liquids and of certain liquid mixtures (*9, 15, 20*). Unfortunately, estimating specific heats of common hydraulic fluids by this approach is very difficult. First, fluids are often compounded from substances of greatly differing molecular type. This results in large heats of mixing and makes unreliable any additive rule for predicting specific heats of fluids from their pure components. There is a dearth of heat capacity data on liquids which are chemically related to the components in many hydraulic fluids. Moreover, the few available values are not in good agreement and do not generally cover a large temperature range.

Therefore, it is necessary to evaluate the specific heats of the hydraulic fluids experimentally.

HYDRAULIC FLUIDS

The three hydraulic fluids investigated are not pure compounds but mixtures compounded for unique and desirable properties (*5*). Aircraft hydraulic fluid MIL-O-5606 is a petroleum base fluid which is recommended for use below 70°C. To date, over 25,000,000 gallons of this fluid have been placed in operation. A typical composition of this fluid is shown in Table I.

Oronite high temperature hydraulic fluid 8200 was developed to provide a fluid with excellent physical properties for use in aircraft at elevated temperatures. The fluid is composed predominantly of a specific alkoxydisiloxane. It contains a silicone thickener which acts as a viscosity index improver.

Table I. Composition of Fluid MIL-O-5606

	Wt. %
Highly treated light gas oil fraction	60–80
Highly treated heavy gas oil fraction	15–30
Polyalkylmethacrylate	4–8
Oxidation inhibitors	0.1–0.5
Red dye	Trace

Oronite high temperature hydraulic fluid 8515 has essentially the same composition as fluid 8200, except that it contains 15% by weight di(2-ethylhexyl) sebacate. This gives fluid 8515 a greater compatibility with rubber in hydraulic systems over the recommended operating range of −54° to 204°C.

METHOD

A differential heating method was chosen for measuring specific heats. This choice was based on the nature of the